Nanoparticle Deposition During Cu-Water Nanofluid Pool Boiling

IOP Conf. Series: Journal of Physics: Conf. Series **923** (2017) 012004 doi:10.1088/1742-6596/923/1/012004

Nanoparticle Deposition During Cu-Water Nanofluid Pool Boiling

L Doretti[1], G A Longo[2], S Mancin[2], G Righetti[2] and J A Weibel[3]

[1]Dept. of Civil, Architectural and Environmental Engineering, University of Padova, Via Venezia 1, 35131, Padova, IT
[2]Dept. of Management and Engineering, University of Padova, Str.lla S. Nicola 3, 36100, Vicenza, IT
[3]School of Mechanical Engineering, Purdue University, 585 Purdue Mall, 47907-2088, West Lafayette, IN

E-mail: tony@gest.unipd.it

Abstract. The present research activity aims to rigorously investigate nanofluid pool boiling in order to definitively assess this as a technique for controlled nanoparticle coating of surfaces, which can enhance the nucleate boiling performance. This paper presents preliminary nanoparticle deposition results obtained during Cu-water (0.13 wt%) nanofluid pool boiling on a smooth copper surface. The tests were run in an experimental setup designed expressly to study water and nanofluid pool boiling. The square test sample block (27.2 mm × 27.2 mm) is equipped with a rake of four calibrated T-type thermocouples each located in a 13.6-mm deep holes drilled every 5 mm from 1 mm below the top surface. The imposed heat flux and wall superheat can be estimated from measurement of the temperature gradient along the four thermocouples. The samples are characterized by scanning electron microscopy (SEM) to analyse the morphological characteristics of the obtained thin, Cu nanoparticle coating.

1. Introduction

Pool boiling is widely used in many different engineering systems: chemical and nuclear reactors, refrigerating and air conditioning equipment, and thermal management of electronic devices. These applications have a shared limitation on the maximum heat flux that can be rejected by the cooling systems under safe, reliable, and efficient operation.

The study of the pool boiling has been a topic of the worldwide research since Nukiyama [1] conducted experiments to develop a boiling curve in stagnant liquid. It is well known that various surface treatment approaches can effectively enhance boiling heat transfer. In particular, microparticle coatings have been experimentally demonstrated to have promising capabilities for the enhancement of nucleate boiling heat transfer coefficients and critical heat flux (CHF).

Recent work has led to new concepts for surface modification at the nanoscale. Over the last decade, nanostructured materials (*e.g.*, nanowire coatings, nanoporous layers, carbon nanotube arrays, *etc.*) have been also shown to enhance nucleate boiling (NB) by several authors [4-6]. A comprehensive review can be found in Ref. [7].

An alternative strategy to enhance boiling heat transfer is by using fluid additives, for example by seeding the fluid with a small concentration of nanoscale particles to produce a nanofluid. The heat

transfer behaviour of nanofluids has been extensively studied by many researchers since the late 1990s. For application of nanofluids under pool boiling conditions, some significant, though quite scattered, enhancements from 10% to 400% of the pool boiling CHF have been reported [8-12]; however, there are also contrasting reports of large deterioration [13-16]. Results in the literature are inconsistent even for the same nanoparticle size/type under similar experimental conditions.

There are a few possible parameters affecting boiling heat transfer with nanofluids, which includes morphological and thermophysical properties of nanoparticles and nanofluids, the stability of nanofluids, the content of nanofluids such as the presence of surfactants and ions, and the deposition and interaction of nanoparticles with the heating surface. As boiling heat transfer is very sensitive to surface characteristics, especially the number and shape of potential nucleation sites, any change in the surface would probably result in different boiling behaviours. There is a general scientific agreement on the fact that the enhancement or the deterioration observed during nanofluid boiling can be attributed to modification of the surface via nanoparticle deposition [17].

The present research activity aims to rigorously investigate nanofluid pool boiling in order to clearly asses the potential of this technique for obtaining either higher CHF values directly or to produce coated surfaces, which can enhance the nucleated boiling performance. This paper presents preliminary nanoparticle deposition results obtained during Cu-water (0.13 wt%) nanofluid pool boiling on a smooth copper surface.

2. Experimental setup and data reduction

As shown in Figure 1, tests are performed in an experimental setup designed and built to study water and nanofluid pool boiling on smooth or enhanced surfaces. In order to avoid any contamination of the components by the nanoparticles contained in the nanofluid, two identical setups were used, one for the pure fluid tests and one for the nanofluid tests.

The heater assembly consists of two heater block sections, both made of copper. The first 19 mm-tall test sample block has the top surface exposed to the working fluid; the second heater block section contains nine electrical cartridge heaters (200 W/240 V) controlled by a motorized Variac for heating of the test sample from below.

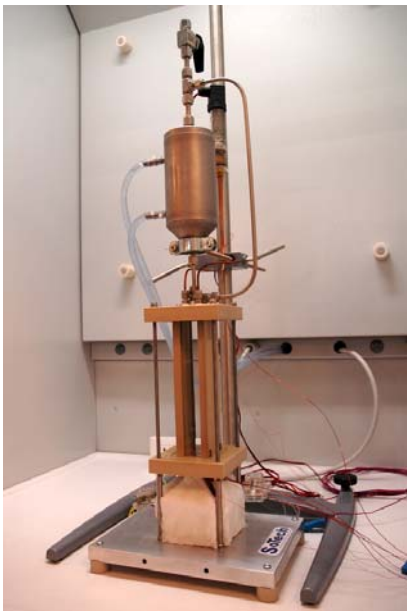

Figure 1. Photograph of the experimental setup. The test chamber for confined boiling experiments is mounted to the top of the heater block assembly.

The test sample block is designed to have a characteristic heater size equal to the Rayleigh-Taylor wavelength, being 27.2 mm in the case of water at ambient conditions. Each test sample block is glued in a polyether ether ketone (PEEK) plate (thermal conductivity, $\lambda = 0.028$ W m^{-1} K^{-1}) and exposes a smooth or enhanced top surface area (27.2 mm × 27.2 mm) to the working fluid (water or nanofluid). Two different boiling chambers were designed to analyse the boiling behaviour in confined and unconfined conditions (*i.e.*, whether the chamber is equal to or larger than the boiling surface, respectively). Both 200 mm-tall chambers consist of two glass and two PEEK walls; sealing is accomplished by means of a silicone o-rings. One chamber has exactly the same cross sectional size of the heating block to study confined pool boiling, while the other has a larger cross section (54.2 mm × 54.2 mm) to study the unconfined pool boiling behaviour. Nanoparticle deposition tests were always run using the confined chamber in order to avoid the contamination of the PEEK plate during the nanofluid boiling, whereas the other two chambers were used for the pure water tests.

Each boiling chamber is closed by a top PEEK plate and the vapour space is directly connected to the condenser, which is located on the top and fed with tap water. There are four threaded holes in the top PEEK plate to allow direct access to the boiling chamber. One hole is used to insert a temperature probe equipped with a T-type thermocouple (uncertainty ±0.05 K, for coverage factor, k = 2) to monitor the fluid temperature 20 mm above the heated surface while another hole is connected to an absolute pressure transducer (uncertainty ±0.065% f.s., f.s. = 20 bar, k = 2) to monitor the saturation pressure. The third hole is used to convey the vapour to the top of the condenser, while the last hole is used to charge the boiling chamber with fluid.

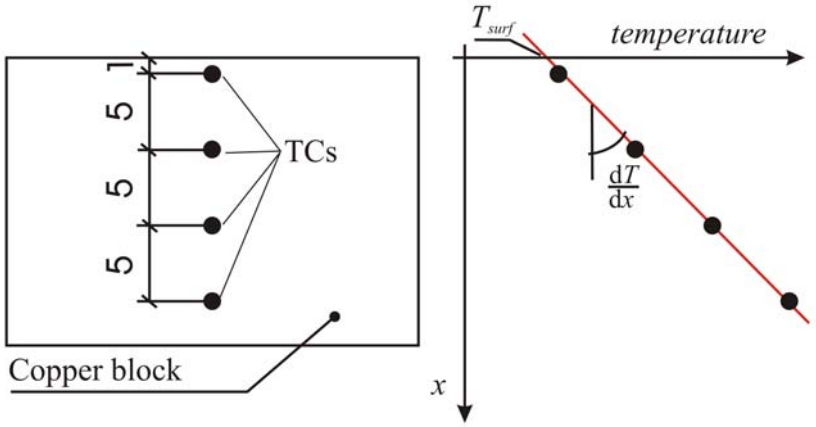

Figure 2. Schematic drawing of the test sample block with thermocouple locations indicated (dimensions in mm), and representative plot the temperature profile along the block height.

As illustrated in Figure 2, the copper test sample block is equipped with four calibrated T-type thermocouples located in as many 13.6 mm-deep holes drilled every 5 mm from 1 mm below the top surface. The imposed heat flux and wall superheat can be estimated from analysis of the temperature gradient measured by the thermocouples. The tests were run by increasing the heat flux up to the point of CHF. The data logging frequency was set at 1 Hz and, at steady state conditions, the experimental data collected over 100 s were time-averaged for subsequent post-processing of the actual surface heat flux and corresponding surface temperature.

In fact, assuming one-dimensional conduction, the temperature along the sample can be approximated by the following expression:

$$T(x) = T_{surf} + \left|\frac{dT}{dx}\right| \cdot x \tag{1}$$

where T_{surf} is the surface temperature at the position $x = 0$, and dT/dx is the temperature gradient estimated by a simple linear regression of the recorded temperatures. Thus, the heat flux q is given by:

$$|q| = \lambda \cdot \left|\frac{\mathrm{d}T}{\mathrm{d}x}\right| \tag{2}$$

where λ is the thermal conductivity of the sample block (387 W m^{-1} K^{-1} for 99.99% pure copper). The wall heat transfer coefficient h can be calculated by dividing the heat flux by the wall superheat, as:

$$h = \frac{q}{T_{surf} - T_{sat}} \tag{3}$$

Four additional calibrated T-type thermocouples were located in the lower heater block section to verify the estimated heat flux. A high-speed video camera is used to visualize the boiling phenomenon through the glass walls.

As described before, the heat flux and the wall temperature are obtained from a linear fit to the temperature data; the uncertainties in the linear fit by a least-squares regression are obtained as described by Brown *et al*. [18]. The surface temperature and heat flux uncertainties are approximately ±0.06 °C and ±4.0 kW/m^2 over the range of heat fluxes investigated.

3. Setup calibration

The experimental setup and procedure were validated through a set of calibration boiling curves obtained for water on a smooth copper sample, using both the confined and unconfined chambers. The copper sample topography was characterized by means of a 3D optical profilometer; Table 1 lists main surface roughness parameters of the sample.

Table 1. Surface roughness parameters of the smooth copper calibration sample according to ISO 4287 [19].

Roughness parameter	Calibration Sample
Ra (arithmetical mean deviation of the roughness profile)	0.070 μm
Rz (maximum height of the roughness profile)	0.695 μm
Rt (total height of the roughness profile)	1.83 μm
RSm (mean width of the roughness profile elements)	82.4 μm

The main results are plotted in Figure 3, which shows a water boiling curve obtained for the smooth copper sample in unconfined conditions. As described before, the tests were run by increasing the heat flux up to the point of CHF (yellow dots in Figure 3), which was found to be 1265 kW m^{-2} for this sample. Figure 3 also reports the value of the CHF as calculated using the well-known Zuber [20] correlation as reported by Lienhard and Dhir [21]:

$$CHF = 1.14 \cdot \frac{\pi}{24} \cdot \sqrt{\rho_V} \cdot h_{LV} \cdot [\sigma \cdot g \cdot (\rho_L - \rho_V)]^{0.25} \tag{4}$$

where the subscripts L and V refer to saturated liquid and vapour, respectively, ρ is the density, h_{LV} is the latent heat of vaporization, σ is the surface tension, and g is the gravitational acceleration.

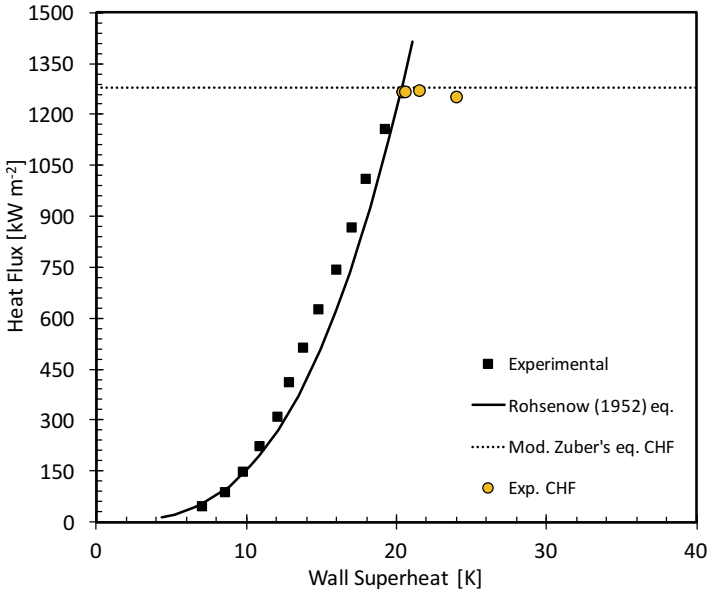

Figure 3. Boiling curve for water on the smooth copper surface in the unconfined test chamber.

When applied to the current experimental test conditions, the calculated CHF is equal to 1283 kW m^{-2}, which is in excellent agreement with the experimental value.
Furthermore, the diagram also reports the values of the heat flux as a function of the wall superheat calculated with the Rohsenow [22] equation:

$$q_{Ro} = \mu_L \cdot h_{LV} \cdot \left[\frac{g\cdot(\rho_L-\rho_V)}{\sigma}\right]^{0.5} \cdot \left(\frac{c_{p,L}\cdot(T_{surf}-T_{sat})}{C_{sf}\cdot h_{LV}\cdot Pr_L}\right)^3 \quad (4)$$

where μ_L, $c_{p,L}$, and Pr_L are the liquid dynamic viscosity, specific heat capacity, and Prandlt number, respectively. C_{sf} is the surface-liquid coefficient, which in this case (i.e. polished copper-water) was taken equal to 0.0128. The results are in fair agreement with the experimental values, showing relative and absolute deviations equal to -27.8% and 35.5%, respectively.

4. Nanoparticle deposition

The nanoparticle deposition was obtained via vigorous boiling of a Cu-water nanofluid obtained by seeding 25 nm copper nanoparticles into distilled pure water. Specifically, 25 g of copper nanoparticles were dispersed in 2 liters of distilled water, obtaining a 1.2 wt% (*i.e.*, 0.13 vol%) Cu-water nanofluid, which was then stirred for 4 hr and sonicated for 3 hr to ensure uniform dispersion.

The surface topography of the smooth copper sample used for the nanoparticle deposition test was also characterized; Table 2 lists the values of the measured roughness parameters. Moreover, the morphology of the surface was further analyzed using scanning electron microscope (SEM) imaging (FEG-ESEM, Quanta 250); a few selected SEM images are shown in Figure 4. Finally, the contact angle measured for a 5 μL water droplet deposited on the smooth copper surface was 88.2 deg ± 2.0 deg.

The experimental campaign consisted of two different tests: the first test investigated pure water boiling performance on the smooth copper surface while the second test was performed with the Cu-water nanofluid to obtain the nanoparticle deposition on the same copper block.

Table 2 Main surface roughness parameters of the smooth copper deposition sample according to ISO 4287 [19].

Roughness parameter	Deposition Sample
Ra	0.054 μm
Rz	0.473 μm
Rt	1.02 μm
RSm	55.6 μm

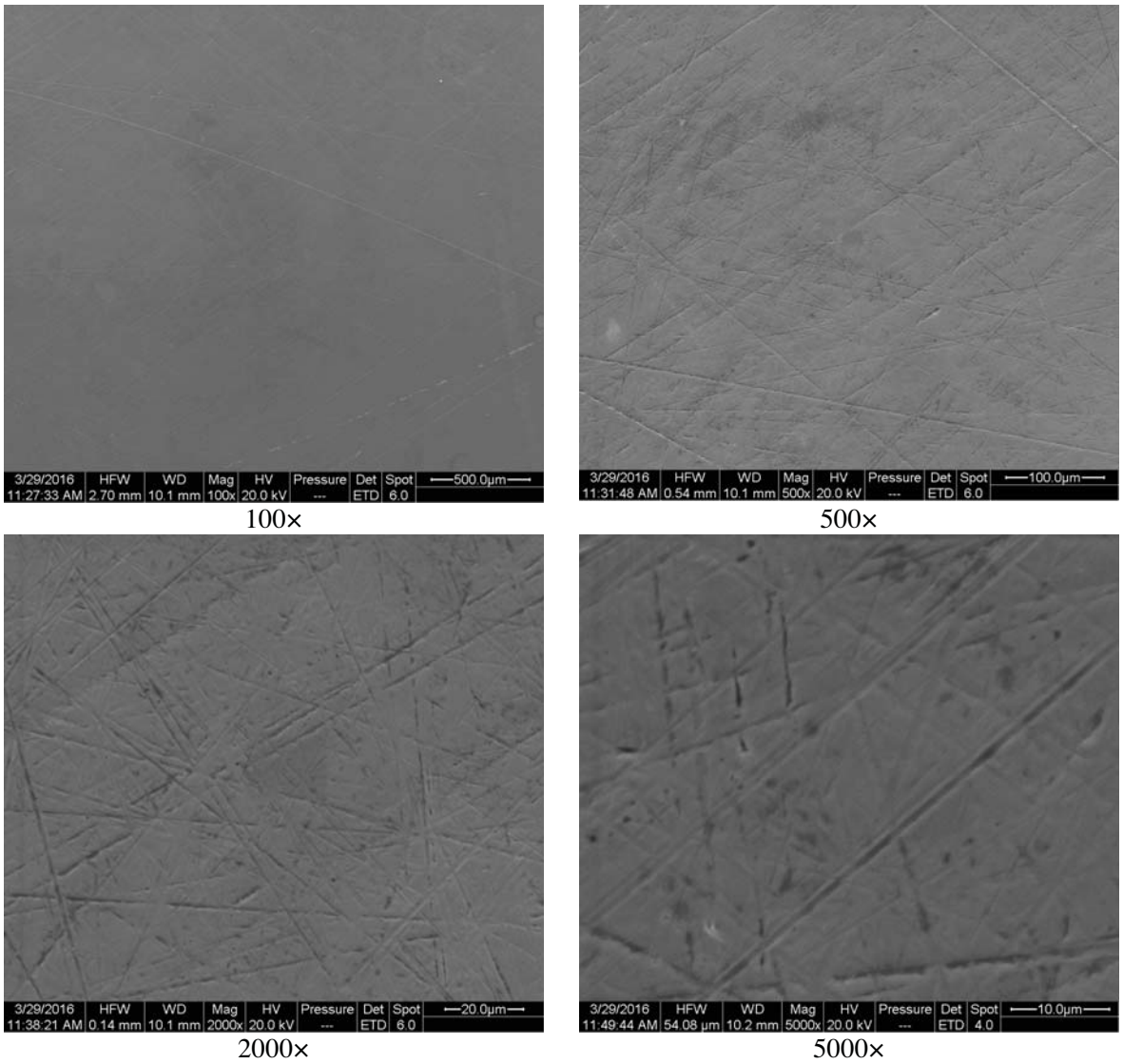

Figure 4. SEM images of the smooth copper surface before nanoparticle deposition.

Figures 5 and 6 report the boiling curves and values of the heat transfer coefficient as a function of heat flux that were measured during the pure water and Cu-water nanofluid pool boiling experiments. As shown in Figure 5, for both tests the heat flux was limited to around 30% of the CHF

observed for the smooth surface to avoid this extreme event. The deposition was performance at approximately 300 kW m^{-2} and 400 kW m^{-2}; at both these heat fluxes, boiling was sustained for 30 min at steady state.

Analysing the results plotted in Figures 5 and 6, it appears that the boiling performance of the Cu-water nanofluid is better as compared to that measured during pure water boiling. In particular, at all the investigated heat fluxes, the associated wall superheats are lower in the case of nanofluid boiling, and thus the heat transfer coefficients are from 15% to 34% greater than those measured during pure water boiling.

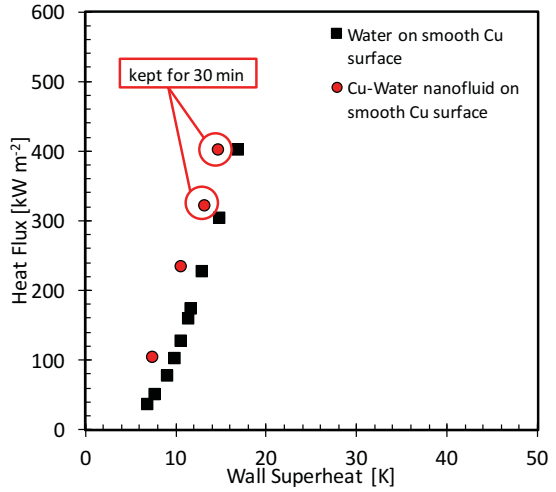

Figure 5. Boiling curve (*i.e.*, heat flux versus wall superheat) for pure water and Cu-water nanofluid boiling.

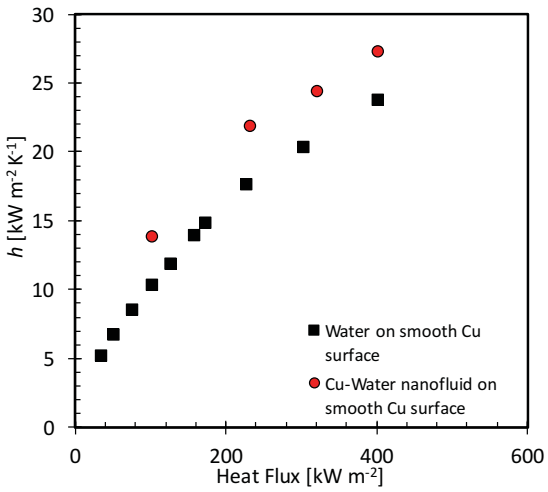

Figure 6. Heat transfer coefficient versus wall superheat for pure water and Cu-water nanofluid boiling.

Figure 7 presents two SEM images of the test surface after Cu-water nanofluid boiling taken at 90× and 100× magnification. The images reveal a thin layer of nanoparticles deposited onto the smooth surface, which is flaking up from the surface in several locations.

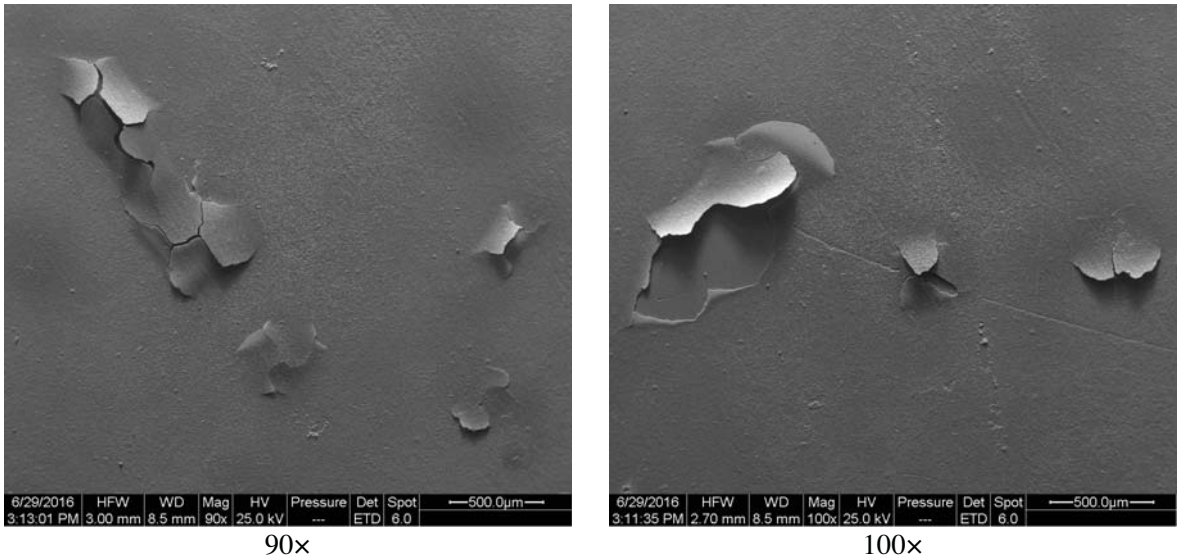

90× 100×

Figure 7. SEM images of the coated copper surface after nanoparticle deposition by boiling of the Cu-water nanofluid.

The observed flaking process might be caused by cleaning of the sample before the SEM imaging procedure. The coating seems to be uniform and smooth, and it follows the topography of the uncoated surface. Figure 8 reports four more SEM images taken at higher magnifications from 1000× to 10000× in order to further inspect the coating.

Considering the first image taken at 1000×, the coating seems to consist of a sublayer of nanoparticles that is relatively uniform and dense; on top of which there is a secondary layer of additional nanoparticles that are more sparsely deposited. This layered deposition structure is more easily recognized in the image taken at higher magnification (5000×). When further zooming in to 10000× magnification, the additional nanoparticles, sparsely deposited, are more evident.

The contact angle measurement was repeated by depositing a 5 μL water droplet on the coated surface. It was found to be 107.9 deg, which is 19.7 deg higher than that measured for the uncoated surface before nanofluid boiling.

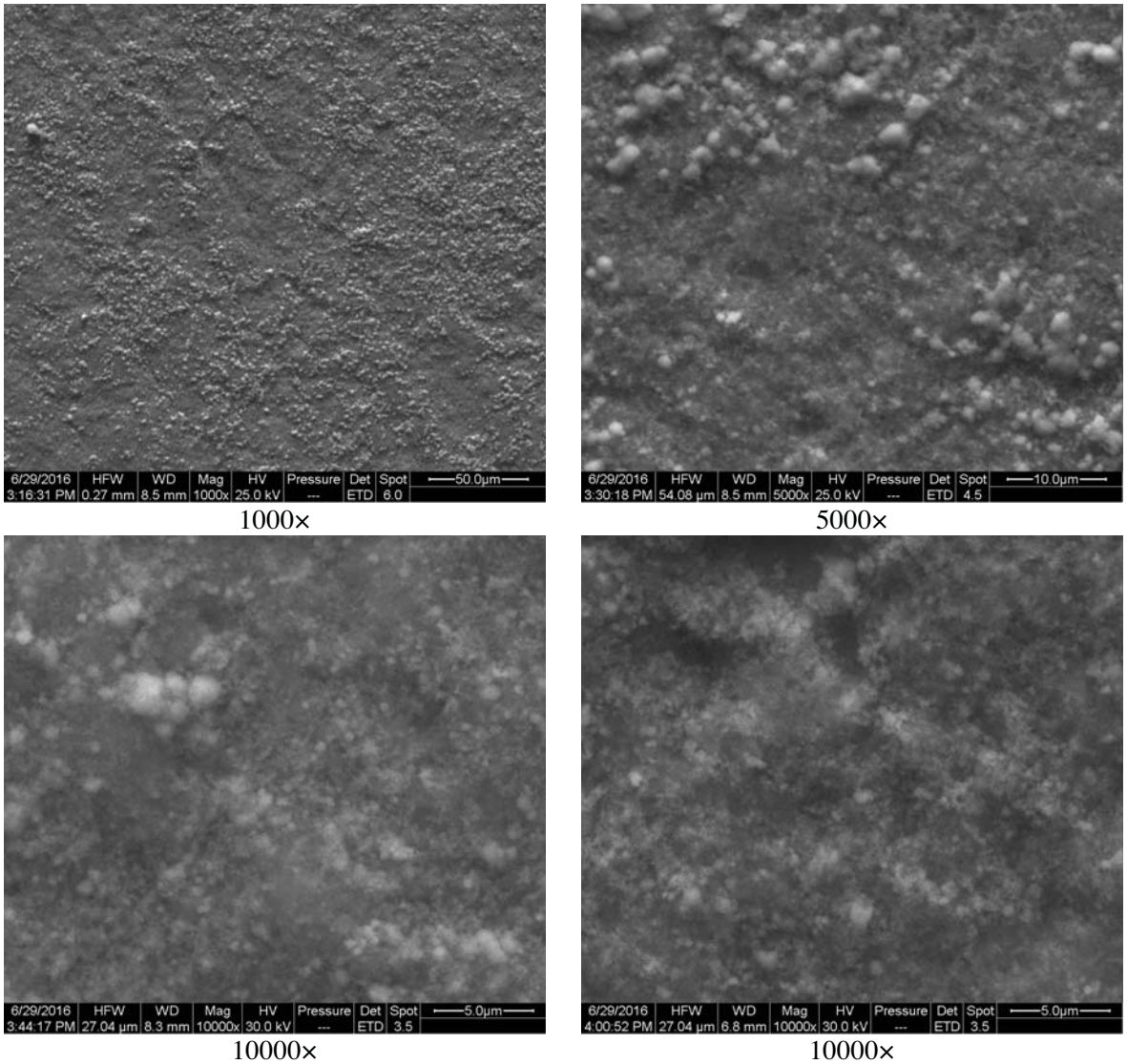

Figure 8. High-magnification SEM images of the coated copper surface after nanoparticle deposition by boiling of the Cu-water nanofluid.

5. Conclusions

This paper presents preliminary nanoparticle deposition results obtained during Cu-water (0.13 wt%) nanofluid pool boiling on a smooth copper surface. The results showed that the Cu-water nanofluid exhibited better boiling heat transfer performance, showing higher heat transfer coefficients as compared to boiling with pure water, on the smooth copper sample. After boiling with the nanofluid, a thin coating was formed on the surface by deposition of the nanoparticles; this coating seems to be uniform, with only a few defects found that might have been caused by post-test cleaning. Scanning electron microscopy images taken of the sample after nanofluid boiling also showed that the coating consists of a dense, uniform bottom layer onto which a secondary nanoparticle deposition occurred, creating another thin more sparsely porous layer. Finally, a contact angle measurement made on both the uncoated and coated surfaces highlighted the effect of the nanoparticle deposition on wetting: in fact, the contact angle increased from 88.2° to 107.9°. These preliminary results show the interesting possibilities offered by the nanofluid boiling as possible new particle deposition technique to realize thin coatings for nucleate boiling enhancement. Further experimental analyses are surely needed to understand the underlying deposition mechanisms in order to develop a rigorous and repeatable deposition protocol.

6. Acknowledgment

This research project was funded by University of Padova through the project CPDA149720: “An Innovative Nanoparticles Deposition Method for Nucleate Boiling Enhancement”. The Authors would thank Eng. Roberto Meneghello and Dr. Enrico Della Rovere for their fundamental contribution to the surface characterization.

7. References

[1] Nukiyama S, 1934 J. *of the Japan Society of Mech. Eng.* **37** (206) 367-374.
[2] Hwang G S and Kaviany M 2006 *Int. J. Heat Mass Transf.* **49** 844-849
[3] Kim J H, Rainey K N, You S M and Pak J Y 2002 *J. Heat Transf*er **124** 500-506.
[4] Lu Y W and Kandlikar S 2011 *Heat Transf. Eng.* **32** (10) 827-842.
[5] Ujereh S, Fisher T, and Mudawar I 2007 *Int. J. Heat Mass Transf.* **50** 4023-4038.
[6] Li S, Furberg R, Toprak M S, Palm B and Muhammed M 2008 *Adv. Funct. Mater.* **18** 2215-2220.
[7] El-Genk M S and Ali A F 2010 *Int. J. Multiphase Flow* **36** 780-792.
[8] Kedzierski 2009 *J. Heat Transfer* **131** 043205.
[9] Park K-J and Jung D 2007 *Int. J. Heat Mass Transf.* **50** 4499-4502
[10] Liu Z, Xiong J and Bao R 2007 *Int. J. Multiphase Flow* **33** 1284-1295.
[11] Park K-J, Jung D and Shim SE 2009 *Int. J. Multiphase Flow* **35** 525-532.
[12] Kathiravan R, Kumar R, Gupta A, and Chandra R, 2009 *J. Heat Transfer* **131** 081902
[13] Trisaksri V and Wongwises S 2009 *Int. J. Heat Mass Transf.* **52** 1582-1588.
[14] Kim H D and Kim MH 2007 *App. Phys. Lett.* **91** 014104.
[15] Bang I C and Chan S H, 2005 *Int. J. Heat Mass Transf.* **48** 2407-2419
[16] Das S K, Putra N, Roetzel W 2003 *Int. J. Heat Mass Transf.* **46** 851-862.
[17] Wen 2012 *Applied Therm. Eng.* **41** 2-9.
[18] Brown K, Coleman H and Steele W 1995 In: *Proceedings of the 33rd Aerospace Science Meeting and Exhibit, Reno, NV, USA.*
[19] International Organization for Standardization, 1997 ISO4287
[20] Zuber N 1952 *Physics and Mathematics* **AECU 4439**.
[21] Lienhard JH and Dhir VK 1973 *National Aeronautics and Space Administration Report* NASA CR-2270
[22] Rohsenow WM 1952 *Transactions of the ASME*, **74**, 969.